

Laser cooling of trapped ions in a standing wave

J. I. Cirac,* R. Blatt,† and P. Zoller

*Joint Institute for Laboratory Astrophysics, University of Colorado, Boulder, Colorado 80309-0440
and Department of Physics, University of Colorado, Boulder, Colorado 80309-0440*

W. D. Phillips

National Institute of Standards and Technology, Gaithersburg, Maryland 20899

(Received 6 March 1992)

Laser cooling of trapped ions in a standing- and running-wave configuration is discussed theoretically. The ions are assumed to be spatially localized on the scale provided by the wavelength of the laser (Lamb-Dicke limit). A master equation for the center-of-mass distribution of the ion is derived for a multilevel system and explicit results are presented for two- and three-level systems and harmonic trapping potentials. For the two-level system located at the node of the standing wave, we find final temperatures that are a factor of 2 lower than the limit for a running wave and cooling rates that do not saturate with the laser intensity. At the point of maximum gradient of the standing wave, blue detuned cooling is found that is analogous to the Sisyphus cooling of free atoms. For a three-level system we compare our results with those of Wineland, Dalibard, and Cohen-Tannoudji [J. Opt. Soc. Am. B **9**, 32 (1992)].

PACS number(s): 32.80 Pj

I. INTRODUCTION

Laser cooling of single trapped ions [1, 2] has been of increasing interest for more than a decade [5–7]. Proposed by Wineland and Dehmelt in 1975 [3], laser cooling was first observed by Neuhauser, Hohenstatt, Toschek and Dehmelt and by Wineland, Drullinger, and Walls in 1978 [4], and started a renewed investigation of the fundamental interaction between electromagnetic radiation and matter with particular emphasis on the coupling between internal (atomic) and external (motional) degrees of freedom. This fundamental interest is due to the fact that a single trapped and cooled ion provides a quantum system close to theoretical models in quantum optics. This feature makes a single trapped and laser-cooled ion the preferred subject for ultrahigh precision spectroscopy and the ultimate candidate for time and frequency standards [1].

On the theoretical side, many aspects of laser cooling of a single trapped ion are well understood [6]. Wineland and Itano [8], and Stenholm, Javanainen, and Lindberg [6, 9, 10] developed theories which allow us to determine laser cooling rates in traps and final energies. In brief, as long as the trap frequency ν is smaller than the natural linewidth Γ of the optical transition for laser cooling (i.e., the weak-binding limit), the final temperature is limited by $T = \hbar\Gamma/2k_B$ where k_B is Boltzmann's constant (Doppler limit). On the other hand, for trap frequencies $\nu > \Gamma$ (i.e., the strong-binding limit), the trapped particle develops well-resolved absorption sidebands at the trap frequency and can be optically pumped to its lowest vibrational state by exciting selectively on the lower sideband (sideband cooling). Experimentally, the residual temperature in this case (given by the residual uncertainty of being in the lowest state) can be very low. Both the Doppler and the sideband limit have been ob-

served in experiments, and agree well with the theoretical predictions [11].

During the past few years significant progress has been made in our understanding of laser cooling of free atoms [12]: aside from the usual cooling by scattering forces, many cooling schemes have been investigated and proved successful, in particular those concerned with dipole forces (in a standing wave) [13]; extremely low temperatures have been achieved with polarization gradient cooling [14] (which is connected to a multilevel Zeeman structure), and dark state cooling [15]. Although laser cooling of trapped ions has been demonstrated previous to cooling of free atoms, these cooling mechanisms and variants have not been investigated for trapped ions. In contrast to studies of free atoms, theoretical and experimental work is mostly restricted to two-level systems. A noticeable exception is experimental and theoretical work on three-level ions where Raman cooling has been predicted to achieve ultimately low temperatures [10], and very recently theoretical work on Sisyphus cooling [16]. Otherwise, there is no work on laser cooling in multilevel systems and standing waves with ion traps.

In the present paper we investigate theoretically laser cooling of trapped ions in a standing-wave (SW) laser field (see also [17]). Since trapped ions can be spatially localized to dimensions smaller than an optical wavelength (Lamb-Dicke limit), cooling can be studied for different positions of the ion within the standing wave. Of particular interest is the cooling dynamics at the node and antinode of the SW, and the point of maximum gradient.

A simple, though not complete, model serves to illustrate one of the features that can arise from such considerations. Take a two-level atom, trapped in the Lamb-Dicke limit, and sideband laser cooled in a standing wave where the node is at the trap center. The tuning of the laser is $\omega_0 - \nu$, the free-atom resonant frequency minus the trap frequency. This resonantly excites, for exam-

ple, transitions from the internal atomic ground state in the first excited trap state to the internal atomic excited state in the fundamental trap state. Subsequent decay to the internal ground state in the trap fundamental state completes a cooling cycle, while off-resonant transitions excited from this lowest-energy state provide the competing heating mechanism. Locating the standing-wave node at the trap center favors the cooling transition over the heating transition because the lowest-energy state is more nearly “in the dark,” having the smallest spatial extent around the node. In this way, a lower temperature is reached compared to the running-wave case where no such spatial advantage is present.

This simplified model cannot predict all the phenomena treated here. Instead, we choose as the tool for our calculation the quantum master equation for laser cooling in the Lamb-Dicke limit, as derived for example by Stenholm and co-workers for two-level systems in running waves (RW) [6, 9]. We generalize this equation to multilevel systems and standing-wave configurations. Furthermore, an essential element of our formulation is the identification of heating and cooling rates in terms of *internal* atomic correlation functions of the quadrature components of the atomic polarization. For a two-level system (TLS) we find that at the node of the SW and for red laser detunings the final energy of the ion is half the Doppler limit. In contrast to the RW configuration, the final energy is independent of the laser intensity, and in addition the cooling rates do not saturate as a function of the Rabi frequency. At the antinode we find only heating.

This general treatment of laser cooling in traps allows one to easily calculate the final energy of a trapped atom for running as well as standing waves or for any other field configuration. For illustration, the master equation is derived for the case of harmonic trapping and it is shown that with the application of standing waves for cooling a trapped ion, the final temperature can be lower than the Doppler limit (which applies for the running wave). This is achieved when the trapped ion is located at the node of the standing wave; at the antinode only heating is obtained. Moreover, when the ion is located near the point of the standing wave’s steepest gradient and the laser is sufficiently intense, cooling is observed for blue detunings instead of red detunings as is the case for usual Doppler and sideband cooling. This is the Sisyphus cooling effect, as has been previously discussed for free atoms [13] and has been recently calculated by Wineland, Dalibard, and Cohen-Tannoudji for a three-level configuration [16].

The paper is organized as follows: In Sec. II the master equation for laser cooling of a multilevel system is derived. In Sec. III we calculate the cooling rates and final temperatures for the RW and SW configurations. A discussion of these results is given in Sec. IV. Finally, in Sec. V laser cooling of a three-level atom in a SW is discussed for a model introduced by Wineland, Dalibard, and Cohen-Tannoudji [16]. The technical details of the adiabatic elimination procedure and a generating function technique for a numerical solution of the full master equation of a two-level atom in a harmonic trap potential are given in Appendixes A and B, respectively.

II. LASER COOLING OF TRAPPED MULTILEVEL IONS IN THE LAMB-DICKE LIMIT

In this section we derive the master equation for laser cooling of trapped multilevel ions in the Lamb-Dicke limit [6, 9]. In this limit the ions are assumed to be well localized on the scale of the laser wavelength, and cooling occurs on a time scale slow in comparison with the internal atomic dynamics. This allows adiabatic elimination of the internal degrees of freedom to derive a master equation for the center-of-mass distribution function of the ion. In previous work [6, 9, 10] this Lamb-Dicke master equation has been derived and solved for two- and three-level systems interacting with a running wave, and for harmonic trapping potentials. Here we will present a derivation for a multilevel system, a general trapping potential and running- and standing-wave configurations. We will show that the transition rates between the levels of the trapping potential, which correspond to laser cooling and heating, can be expressed in terms of correlation functions of quadrature components of the atomic polarization operators. For a harmonic trapping potential these rates can be interpreted as the absorption spectrum of motion-induced sidebands of the laser fields.

A. Master equation for the multilevel system

We consider an ion trapped in a potential. The ion interacts with laser light and is damped by spontaneous emission. For simplicity we will restrict ourselves to a one-dimensional atomic motion. The master equation for the reduced system density operator ρ , which is obtained by tracing over the empty modes of the radiation field, obeys the equation ($\hbar = 1$) [6]

$$\frac{d}{dt}\rho = -i[H_{\text{tp}} + H_I + V_{\text{dip}}, \rho] + \mathcal{L}^d \rho. \quad (1)$$

Here, H_{tp} is the Hamiltonian for the center-of-mass motion of the ion in the trap (external degrees of freedom); it is a function of the momentum \hat{P} and position operator \hat{R} of the ion. H_I is the free Hamiltonian for the internal energy levels of the ion, and V_{dip} describes the dipole interaction of the laser with the ion. Damping by spontaneous emission is contained in the Liouvillian \mathcal{L}^d , given by

$$\mathcal{L}^d \rho = \sum_{i,j} \gamma_{ji} (2\sigma_{j,i} \tilde{\rho}_{ij} \sigma_{i,j} - \sigma_{i,j} \sigma_{j,i} \rho - \rho \sigma_{i,j} \sigma_{j,i}), \quad (2)$$

where $2\gamma_{ji}$ is the spontaneous emission rate $|i\rangle \rightarrow |j\rangle$, and $\sigma_{j,i} = |j\rangle\langle i|$ is the corresponding atomic transition operator. The term

$$\tilde{\rho}_{ij} = \frac{1}{2} \int_{-1}^1 dx W(x) e^{ik_{ij} \hat{R} x} \rho e^{-ik_{ij} \hat{R} x}, \quad (3)$$

accounts for the momentum transfer in emission of a spontaneous photon with momentum $\hbar k_{ij}$ in the decay from the level $|i\rangle$ to $|j\rangle$. $W(x)$ is the angular distribution of spontaneous emission which for a dipole transition is $W(x) = \frac{3}{4}(1+x^2)$.

In the Lamb-Dicke limit (LDL), the motion of the

ion in the trap is confined to a spatial region much smaller than the dimension of the optical wavelength of the exciting laser light. This allows an expansion of the dipole interaction in powers of the small parameter $\eta = \pi a_0/\lambda \ll 1$ where a_0 is the dimension of the ground state of the trap, and λ is the optical wavelength. Expanding the laser-atom interaction around the trap center $R = 0$, we write

$$V_{\text{dip}}(\hat{R}) = V_{\text{dip}}(0) - \hat{R}F - \frac{1}{2}\hat{R}^2F' + \dots, \quad (4)$$

keeping terms up to second order in η . Here F is the gradient of the dipole interaction at $R = 0$, and F' is the second-order derivative. Note that $V_{\text{dip}}(0)$, F , and F' are atomic operators referring only to *internal* atomic degrees of freedom. In a similar way we expand the term $\tilde{\rho}_{ij}$ in the Liouville operator (2). We find

$$\mathcal{L}^d = \mathcal{L}_0^d + \mathcal{L}_2^d + \dots, \quad (5)$$

where

$$\mathcal{L}_0^d \rho = \sum_{j,i} \gamma_{ji} (2\sigma_{j,i} \rho \sigma_{i,j} - \sigma_{i,j} \sigma_{j,i} \rho - \rho \sigma_{i,j} \sigma_{j,i}) \quad (6)$$

is the usual damping term in the atomic master equation when atomic motion is neglected, and

$$\mathcal{L}_2^d \rho = \alpha \sum_{i,j} \gamma_{ji} k_{ij}^2 \sigma_{i,j} (2\hat{R}\rho\hat{R} - \hat{R}^2\rho - \rho\hat{R}^2) \sigma_{j,i} \quad (7)$$

describes the diffusion due to spontaneous emission. In obtaining \mathcal{L}_2^d we have used that the angular distribution for spontaneous emission $W(x)$ is normalized and an even function of x , and have defined

$$\alpha = \frac{1}{2} \int_{-1}^1 dx x^2 W(x),$$

which equals $\frac{2}{5}$ for usual dipole transitions.

Summarizing, we write master equation (1) in the LDL including terms up to second order in η as

$$\frac{d}{dt} \rho = (\mathcal{L}_0 + \mathcal{L}_1 + \mathcal{L}_2) \rho, \quad (8)$$

where

$$\begin{aligned} \mathcal{L}_0 \rho &= -i[H_{\text{tp}}, \rho] + \{-i[H_I + V_{\text{dip}}(0), \rho] + \mathcal{L}_0^d \rho\} \\ &\equiv (\mathcal{L}_{0E} + \mathcal{L}_{0I}) \rho \end{aligned} \quad (9)$$

$$\begin{aligned} \mathcal{L}_1 \rho &= -i[-F\hat{R}, \rho], \\ &= -F(-i[\hat{R}, \rho]) + (i[F, \rho])\hat{R} \\ &\equiv -F(\mathcal{L}_{1E}\rho) + (\mathcal{L}_{1I}\rho)\hat{R}, \end{aligned} \quad (10)$$

$$\mathcal{L}_2 \rho = \frac{i}{2} [\hat{R}^2 F', \rho] + \mathcal{L}_2^d \rho, \quad (11)$$

are the zeroth-, first-, and second-order Liouvillians, respectively. In zeroth order in η Eq. (8) reduces to

$$\frac{d}{dt} \rho = \mathcal{L}_0 \rho \equiv (\mathcal{L}_{0E} + \mathcal{L}_{0I}) \rho. \quad (12)$$

The equation describes the (undamped) motion of the ion

in the trap according to H_{tp} . For the internal degrees of freedom Eq. (12) agrees with the usual atomic master equation for a multilevel atom undergoing spontaneous emission. In order η^0 the internal and external dynamics of the ion are decoupled, and there are no mechanical light effects. Laser cooling of the ion is contained in the interaction terms \mathcal{L}_1 and \mathcal{L}_2 . In view of the smallness of η the coupling between the internal and external degrees of freedom (i.e., the laser cooling) is slow compared with the time scale of the internal atomic dynamics in the LDL. This allows adiabatic elimination of the internal degrees of freedom.

Formally, the adiabatic elimination [6, 9, 18] of the internal degrees of freedom can be achieved as follows. Let us consider the eigenvalue spectrum of the Liouville operator on the right-hand side of the master equation (8). To zero order in the Lamb-Dicke parameter η the eigenvectors of \mathcal{L}_0 with zero eigenvalue $\lambda_0 = 0$ are

$$\mathcal{L}_0 |n\rangle \langle n| \otimes \rho_{\text{SS}} = 0 \quad (n = 0, 1, \dots) \quad (13)$$

with $|n\rangle$ with $n = 0, 1, \dots$ eigenstates of the trap Hamiltonian, $H_{\text{tp}}|n\rangle = \nu_n|n\rangle$, and ρ_{SS} the stationary solution of the atomic density matrix for the internal atomic dynamics, $\mathcal{L}_{0I}\rho_{\text{SS}} = 0$. The subspace spanned by these Liouville eigenvectors is infinitely degenerate. The “excited” nonzero (complex) eigenvalues λ_k ($k = 1, 2, \dots$) of \mathcal{L}_0 will be of the order of multiples of the trap frequency, and the frequency scale of the internal atomic dynamics (the Rabi frequency, spontaneous transition rates, etc.). The zero-order Liouville eigenstates corresponding to $\lambda_0 = 0$ are connected by the operators \mathcal{L}_1 and \mathcal{L}_2 to the subspaces associated with $\lambda_k \neq 0$. This corresponds to a coupling between the internal and external degrees of freedom. To the extent that the laser cooling rate is slow compared with both the trap frequency and the internal atomic frequencies (i.e., $\eta \ll 1$), the coupling between these blocks of eigenvalues and Liouville subspaces of \mathcal{L}_0 is weak and can be described in perturbation theory. We define a projection operator \mathcal{P} on the subspace with zero eigenvalue $\lambda_0 = 0$ of \mathcal{L}_0 according to

$$\mathcal{P} \rho \equiv \mathcal{P}^e \otimes \mathcal{P}^i \rho, \quad (14)$$

with

$$\mathcal{P}^e X = \sum_{n=0}^{\infty} |n\rangle \langle n| \langle n| X |n\rangle \quad (15)$$

the projection operator on the trap populations, and

$$\mathcal{P}^i X = \lim_{t \rightarrow \infty} e^{\mathcal{L}_{0I} t} X \equiv \rho_{\text{SS}} \text{Tr}_I X, \quad (16)$$

the projection operator on the internal stationary atomic density matrix ρ_{SS} ($\text{Tr}_I \dots$ is the trace over the internal degrees of freedom). Projection of the master equation on the \mathcal{P} space gives in second-order perturbation theory in η

$$\frac{d}{dt} \mathcal{P} \rho = [\mathcal{P} \mathcal{L}_2 \mathcal{P} + \mathcal{P} \mathcal{L}_1 (-\mathcal{L}_0)^{-1} \mathcal{L}_1 \mathcal{P}] \rho. \quad (17)$$

This is the required equation of motion for the reduced

density operator

$$\mathcal{P}\rho = \mathcal{P}^e \rho_{\text{SS}} \text{Tr}_I \rho \equiv \rho_{\text{SS}} \mu \quad (18)$$

with $\mu = \text{Tr}_I(\rho)$ a density operator for the center-of-mass

$$\begin{aligned} \frac{d}{dt} \mu = \mathcal{P}^e \left(\frac{i}{2} \langle F' \rangle_{\text{SS}} [\hat{R}^2, (\mathcal{P}^e \mu)] + \alpha \sum_{ij} \gamma_{ji} k_{ij}^2 \langle \sigma_{i,i} \rangle_{\text{SS}} [2\hat{R}(\mathcal{P}^e \mu)\hat{R} - \hat{R}^2(\mathcal{P}^e \mu) - (\mathcal{P}^e \mu)\hat{R}^2] \right. \\ \left. - \int_0^\infty dt \langle F(t)F(0) \rangle_{\text{SS}} [\hat{R}, [\hat{R}(t), (\mathcal{P}^e \mu)]] - \int_0^\infty dt \langle [F(t), F(0)] \rangle_{\text{SS}} [\hat{R}, (\mathcal{P}^e \mu)\hat{R}(t)] \right), \quad (19) \end{aligned}$$

where

$$\hat{R}(t) = e^{\mathcal{L}_{0E} t} \hat{R} \equiv e^{-iH_{\text{tp}} t} \hat{R} e^{iH_{\text{tp}} t}, \quad (20)$$

$$= \sum_{n,n'} |n\rangle \langle n| \hat{R} |n'\rangle \langle n'| e^{-i(\nu_n - \nu_{n'}) t} \quad (21)$$

is the Heisenberg operator for the ion position \hat{R} , and $\langle \cdot \rangle_{\text{SS}}$ stands for the atomic mean values in the steady state ρ_{SS} . The first term on the right-hand side of (19) is a correction to the trap Hamiltonian H_{tp} (a frequency shift), and is usually not of interest. The second term describes the diffusion due to spontaneous emission (with k_{ij} the wave vector for the transition i, j). The last two terms involve the autocorrelation spectrum of the dipole force F at $R = 0$ evaluated at the transition frequencies $\nu_n - \nu_{n'}$ of the trap eigenstates. These terms describe the light-induced transition rates between the trap states $|n\rangle$. Both $\langle F(t)F(0) \rangle_{\text{SS}}$ and $\langle [F(t), F(0)] \rangle_{\text{SS}}$ are atomic correlation functions for the atomic operators F which refer only to the *internal atomic dynamics* and can be evaluated using the quantum regression theorem [18] for optical Bloch equations,

$$\langle F(t)F(0) \rangle_{\text{SS}} = \text{Tr}_I (F e^{\mathcal{L}_{0I} t} F \rho_{\text{SS}}) \quad (22)$$

$$\langle [F(t), F(0)] \rangle_{\text{SS}} = \text{Tr}_I (F e^{\mathcal{L}_{0I} t} [F, \rho_{\text{SS}}]).$$

To summarize, laser cooling of trapped ions in the LDL can be solved in two independent steps: (i) we calculate the cooling and heating rates in Eq. (19) from the Fourier transform of the correlation functions of the internal atomic operator F , which is the gradient of the dipole interaction at the position of the ion; and (ii) we solve the rate equations (17) for the trap populations for the given transition rates.

B. Harmonic trapping

A simple, but particularly interesting case is a harmonic trapping potential described by the Hamiltonian

$$H_{\text{tp}} = \frac{\hat{P}^2}{2M} + \frac{1}{2} M \nu^2 \hat{R}^2 \equiv \nu (a^\dagger a + \frac{1}{2}), \quad (23)$$

where M is the ion mass, ν is the oscillator frequency of oscillations of the ion around $R = 0$, and we have defined

degrees of freedom. In writing Eq. (17) we have made the simplifying assumption that $\mathcal{P}\mathcal{L}_1\mathcal{P} = 0$, which is fulfilled for cases of interest below.

In Appendix A we show that Eq. (17) can be rewritten as

lowering and raising operators according to

$$\hat{R} = \frac{1}{\sqrt{2M\nu}} (a^\dagger + a), \quad \hat{P} = i\sqrt{\frac{M\nu}{2}} (a^\dagger - a). \quad (24)$$

Eigenstates of H_{tp} are the Fock states $|n\rangle$ with energy eigenvalues $E_n = \nu(n + \frac{1}{2})$. The eigenvalues and eigenstates of the Liouvillian \mathcal{L}_{0E} are $i\nu k$ and $|n\rangle \langle n+k|$, respectively, with $k = 0, \pm 1, \pm 2, \dots$. A projection operator \mathcal{P}_k^e on the subspaces associated with these Liouville eigenvalues can be easily defined according to

$$\mathcal{P}_k^e \rho = \sum_{n=0}^{\infty} |n\rangle \langle n+k| \langle n|\rho|n+k\rangle. \quad (25)$$

It can be readily checked that in the present case the condition $\mathcal{P}\mathcal{L}_1\mathcal{P} = 0$ is fulfilled in view of $\langle n|\mathcal{L}_1|n\rangle = 0$. In Appendix A we show that master equation (19) can be written as

$$\begin{aligned} \frac{d}{dt} \mu = -i \left(\nu - \frac{1}{2M\nu} \langle F' \rangle_{\text{SS}} \right) [a^\dagger a, \mu] \\ + \{ \{ [S(\nu) + D] (a\mu a^\dagger - a^\dagger a\mu) \\ + [S(-\nu) + D] (a^\dagger \mu a - a a^\dagger \mu) \} + \text{H.c.} \} \quad (26) \end{aligned}$$

with $S(\nu)$ the fluctuation spectrum of the operator $F(t)$,

$$S(\nu) = \frac{1}{2M\nu} \int_0^\infty dt e^{i\nu t} \langle F(t)F(0) \rangle_{\text{SS}}, \quad (27)$$

and

$$D = \alpha \sum_{i,j}' \langle \sigma_{ii} \rangle_{\text{SS}} \gamma_{ij} \eta_{ij}^2, \quad (28)$$

the diffusion coefficient due to spontaneous emission from the excited atomic states. $\eta_{ij} = k_{ij}/\sqrt{2M\nu}$ (with i, j labeling the atomic transition) are the (small) LDL parameters. Equation (28) is proportional to terms $\langle \sigma_{ii} \rangle_{\text{SS}} \gamma_{ij}$ that are the spontaneous emission rates from the level $|i\rangle$ to $|j\rangle$. Finally, the term involving $\langle F' \rangle_{\text{SS}}$ is a renormalization of the harmonic-oscillator frequency ν due to the presence of the laser field. It is a small correction (of the second order in η) and will be ignored in the following discussion. Equation (26) is the familiar master equation for a damped harmonic oscillator interacting with a finite-temperature heat bath [19].

Taking diagonal matrix elements in the basis of the Fock states $|n\rangle$, we have [6]

$$\frac{d}{dt}p_n = (n+1)A_-p_{n+1} - [(n+1)A_+ + nA_-]p_n + nA_+p_{n-1}, \quad (29)$$

for the populations $p_n = \langle n|\rho|n\rangle$ with transition rates A_\pm given by

$$\begin{aligned} A_- &= 2 \operatorname{Re}[S(\nu) + D], \\ A_+ &= 2 \operatorname{Re}[S(-\nu) + D]. \end{aligned} \quad (30)$$

Equation (29) is identical to the standard cooling master equation for a TLS interacting with a RW (although here the expression of the transition rates A_\pm is general). Thus, the solutions and interpretations given in Ref. [6] for Eq. (29) apply also to the present case. The mean value $\langle n \rangle$ obeys the equation

$$\frac{d}{dt}\langle n \rangle = -(A_- - A_+)\langle n \rangle + A_+ \quad (31)$$

so that we identify $W = A_- - A_+$ with the cooling rate. Cooling occurs for $W > 0$. The corresponding final energy is

$$\begin{aligned} E_{\text{SS}} &= \nu (\langle a^\dagger a \rangle_{\text{SS}} + \frac{1}{2}) \\ &= \nu \left(\frac{A_+}{A_- - A_+} + \frac{1}{2} \right) \quad (W > 0). \end{aligned} \quad (32)$$

III. A_\pm RATES FOR A TWO-LEVEL SYSTEM IN RUNNING AND STANDING WAVES

Here we derive explicit expressions for the rates A_- and A_+ [Eq. (30)] for a two-level system in a running and standing wave. Our results for the running wave coincide with those derived by Stenholm and co-workers [6, 9] derived by somewhat different methods. A detailed discussion of the predictions for the standing wave and its comparison with the results for the running wave will be given in Sec. IV.

A. Running wave

For cooling in a RW the interaction term in the Hamiltonian may be written in a frame rotating at the laser frequency ω_L as

$$V_{\text{dip}}(\hat{R}) = \frac{\Omega_0}{2} \left(\sigma^+ e^{-ik_L \hat{R}} + \sigma^- e^{ik_L \hat{R}} \right), \quad (33)$$

where σ are the usual pseudospin operators for a TLS, Ω_0 is the Rabi frequency for the TLS-laser interaction, and $k_L = \omega_L/c$. According to Eq. (4) one finds for the interaction of the laser with the internal degrees of freedom

$$H_{0I} \equiv H_I + V_{\text{dip}}(0) = -\frac{\Delta}{2}\sigma_z + \frac{\Omega_0}{2}\sigma_x, \quad (34)$$

and for the operator F ,

$$F = -\frac{\Omega_0}{2}k_L\sigma_y. \quad (35)$$

Here $\sigma_x = \sigma^+ + \sigma^-$, $\sigma_y = (\sigma^+ - \sigma^-)/i$, and σ_z are the three components of the Bloch vector, $\Delta = \omega_L - \omega_0$ is the detuning between the laser and the TLS transition frequency, and Ω_0 is the Rabi frequency. Note that in the present case of a running wave the operator F is proportional to the atomic polarization component σ_y . This is related to the fact that the ionic motion in a RW corresponds to a *phase modulation* of the laser field. In order to determine the rates A_\pm [Eq. (30)] we calculate the fluctuation spectrum (27) of the operator $F(t)$,

$$S(\nu) = \eta^2 \left(\frac{\Omega_0}{2} \right)^2 \int_0^\infty dt e^{i\nu t} \langle \sigma_y(t) \sigma_y(0) \rangle, \quad (36)$$

according to the quantum fluctuation regression theorem. For the Bloch equations of a TLS at rest we have

$$\begin{aligned} \frac{d}{dt}\langle \sigma_x \rangle &= -\gamma\langle \sigma_x \rangle + \Delta\langle \sigma_y \rangle, \\ \frac{d}{dt}\langle \sigma_y \rangle &= -\Delta\langle \sigma_x \rangle - \gamma\langle \sigma_y \rangle - \Omega_0\langle \sigma_z \rangle, \\ \frac{d}{dt}\langle \sigma_z \rangle &= \Omega_0\langle \sigma_y \rangle - 2\gamma\langle \sigma_z \rangle - 2\gamma. \end{aligned} \quad (37)$$

Here, $\Gamma = 2\gamma$ is the spontaneous decay rate. The steady-state solutions to these Bloch equations are

$$\begin{aligned} \langle \sigma_x \rangle_{\text{SS}} &= \Omega_0\Delta/P, \\ \langle \sigma_y \rangle_{\text{SS}} &= \gamma\Omega_0/P, \\ \langle \sigma_z \rangle_{\text{SS}} &= -(\gamma^2 + \Delta^2)/P, \end{aligned} \quad (38)$$

where $P = \gamma^2 + \Delta^2 + \Omega_0^2/2$. For Eq. (36) we find

$$\begin{aligned} S(\nu) &= \eta^2 \left(\frac{\Omega_0}{2} \right)^2 \frac{1}{\mathcal{D}} \\ &\quad \times 2\gamma\Omega_0(-i\nu + \gamma)\langle \sigma_y \rangle_{\text{SS}} - \nu\Delta(-i\nu + 2\gamma)\langle \sigma_z \rangle_{\text{SS}} \\ &\quad - i\nu(-i\nu + \gamma)(-i\nu + 2\gamma) + \nu\Omega_0(-i\nu + \gamma)\langle \sigma_x \rangle_{\text{SS}}, \end{aligned} \quad (39)$$

where

$$\begin{aligned} \mathcal{D} &= -i\nu[(-i\nu + \gamma)^2(-i\nu + 2\gamma) \\ &\quad + \Delta^2(-i\nu + 2\gamma) + \Omega_0^2(-i\nu + \gamma)]. \end{aligned} \quad (40)$$

Furthermore, the diffusion coefficient defined in (28) is

$$D = \alpha\eta^2\gamma(1 + \langle \sigma_z \rangle_{\text{SS}})/2 = \frac{1}{4}\alpha\eta^2\gamma\Omega_0^2/P. \quad (41)$$

Substituting (41) and (39) in (30) gives the rates A_- and A_+ . One can show that these rates coincide with results derived earlier by Stenholm and co-workers [9].

B. Standing wave

In a standing wave the laser-atom interaction is

$$V_{\text{dip}}(\hat{R}) = \frac{\Omega_0}{2} \cos(k_L \hat{R} + \varphi)\sigma_x, \quad (42)$$

where φ accounts for the relative position of the ion in the SW. In particular, $\varphi = \pi/2$ corresponds to an ion

centered at a node of the SW, $\varphi = \pi/4$ is the position of the maximum gradient, and $\varphi = 0$ characterizes the position at an antinode. According to Eq. (4) we find

$$H_{0I} = -\frac{\Delta}{2}\sigma_z + \frac{\Omega_0 \cos(\varphi)}{2}\sigma_x, \quad (43)$$

$$F = -\frac{\Omega_0 \sin \varphi}{2}k_L\sigma_x.$$

Note that the effective Rabi frequency $\Omega_\varphi = \Omega_0 \cos \varphi$ for a TLS at rest depends on the relative position φ of the ion in the SW. In particular, we have $\Omega_{\varphi=\pi/2} = 0$, $\Omega_{\varphi=\pi/4} = \Omega_0/\sqrt{2}$, and $\Omega_{\varphi=0} = \Omega_0$. On the other hand, the operator F scales with $\sin(\varphi)$. Furthermore, F is proportional to the polarization component σ_x which mirrors the fact that in the reference frame of the ion the laser appears *amplitude modulated*. We find

$$S(\nu) = \eta^2 \left(\frac{\Omega_0 \sin \varphi}{2} \right)^2 \int_0^\infty dt e^{i\nu t} \langle \sigma_x(t) \sigma_x(0) \rangle, \quad (44)$$

which can be calculated again by the quantum fluctuation regression theorem. The Bloch equations for this case are the same as for a RW (37) with Ω_0 replaced by Ω_φ . For the fluctuation spectrum we have

$$S(\nu) = \eta^2 \left(\frac{\Omega_0 \sin \varphi}{2} \right)^2 \frac{1}{D} \{ 2\gamma\Omega_\varphi\Delta \langle \sigma_x \rangle_{SS} - i\nu[\Omega_\varphi^2 + (-i\nu + \gamma)(-i\nu + 2\gamma)] - \nu\Delta(-i\nu + 2\gamma) \langle \sigma_z \rangle_{SS} - \nu\Delta\Omega_\varphi \langle \sigma_y \rangle_{SS} \}, \quad (45)$$

where D (with $\Omega_0 \rightarrow \Omega_\varphi$) has been defined in Eq. (40). The diffusion coefficient D is again given by Eq. (41). This completes the calculation of the A_\pm rates.

For a SW the cooling rate $W = A_- - A_+$ can be written as

$$W = 2 \left(\frac{g}{2} \right)^2 \text{Re} \left[\int_0^\infty dt e^{i\nu t} \langle \sigma_x(t) \sigma_x(0) \rangle_{SS} - \int_0^\infty dt e^{-i\nu t} \langle \sigma_x(t) \sigma_x(0) \rangle_{SS} \right] = 2 \left(\frac{g}{2} \right)^2 \text{Re} \int_0^\infty dt e^{i\nu t} \langle [\sigma_x(t), \sigma_x(0)] \rangle_{SS} \quad (46)$$

with $g = \eta\Omega_0 \sin \varphi$. In the following we interpret this result from a different perspective. We rewrite the Hamiltonian part of the master equation (1) in an interaction picture with respect to the ion motion (the Hamiltonian H_{tp}). This corresponds to a transformation to the rest frame of the ion. With $a = \tilde{a}e^{-i\nu t}$ and $a^\dagger = \tilde{a}^\dagger e^{i\nu t}$, and in first order in the LDL expansion, we arrive in at

$$H = \frac{1}{2}\omega_0\sigma_z + \frac{\Omega_\varphi}{2}(\sigma^+ e^{-i\omega_L t} + \sigma^- e^{i\omega_L t}) + \frac{g}{2} \{ \sigma^+ [\tilde{a}e^{-i(\omega_L + \nu)t} + \tilde{a}^\dagger e^{-i(\omega_L - \nu)t}] + \text{H.c.} \}. \quad (47)$$

This Hamiltonian describes the interaction of a TLS (at rest) with a laser at frequency ω_L which has two side-

bands at frequencies $\omega_L \pm \nu$. The laser corresponds to a (strong) pump field. In the LDL we have $\eta \ll 1$ and the sidebands can be considered as weak probe fields. Note that the amplitude of the sidebands is proportional to the quantum-mechanical operators \tilde{a} and \tilde{a}^\dagger , and the two sidebands are correlated: for a SW the sidebands are in phase, corresponding to amplitude modulation of the laser (for a RW these sidebands would be out of phase, corresponding to phase modulation).

Coming back to the cooling rate and using the explicit form of σ_x in terms of σ^\pm , we may write

$$W = A_- - A_+ = A(\nu) - A(-\nu), \quad (48)$$

where

$$A(\nu) = g^2 \text{Re} \int_0^\infty dt e^{i\nu t} \langle [\sigma^-(t), \sigma^+(0)] \rangle_{SS} + g^2 \text{Re} \int_0^\infty dt e^{i\nu t} \langle [\sigma^-(t), \sigma^-(0)] \rangle_{SS}. \quad (49)$$

The first term is the usual absorption coefficient for a probe beam of frequency $\omega_L + \nu$. The second term is related to the absorption coefficient, appearing in three-wave mixing due to correlations in the absorption (or emission) of two photons of frequency ω_L and subsequent emission (absorption) of one photon of frequency $\omega_L + \nu$ and another of $\omega_L - \nu$, when the three lasers are in phase. Hence, $A(\nu)$ is the classical absorption-gain coefficient for photons of frequency $\omega_L + \nu$, while $A(-\nu)$ is the same for photons of frequency $\omega_L - \nu$. Then, the cooling condition implies $A(\nu) > A(-\nu)$.

Hence, we conclude that laser cooling can be analyzed in terms of the absorption coefficients for a TLS. This procedure can be extended to the multilevel case by taking into account the corresponding sidebands on all cooling transitions. The absorption spectrum of a TLS in a probe fields with frequencies $\omega_L \pm \nu$ and a pump field of frequency ω_L is discussed in some detail by Meystre and Sargent [20].

IV. LASER COOLING OF A TWO-LEVEL SYSTEM IN A STANDING WAVE: DISCUSSION

In Sec. III we have calculated cooling rates and final temperatures of a single trapped ion in a given wave pattern. Here we present a discussion of numerical results for a SW and compare it to a RW. It has been demonstrated that sideband cooling of trapped ions with a RW makes it possible to reach the lowest vibrational eigenstate $|n=0\rangle$ [11]. Therefore, it is of experimental interest to investigate how far laser cooling in a standing wave leads to lower temperatures and higher cooling rates, especially when the trap frequency is smaller than the natural linewidth (i.e., weak binding limit) which is most often realized in experiments with trapped ions.

Figure 1 shows a comparison of the cooling rates $W = A_- - A_+$ and the final energies $\langle n \rangle$ for the standing-wave case at $\varphi = \pi/2$ [node of SW, Figs. 1(a) and 1(b)] and $\varphi = \pi/4$ [point of maximum gradient, Figs. 1(c) and 1(d)], and for the RW [Figs. 1(e) and 1(f)] for three dif-

ferent Rabi frequencies $\Omega_0 = 0.5, 1$, and 2Γ as a function of the laser detuning Δ/Γ . For the RW [cf. Fig. 1(e)] we obtain the usual dispersive behavior for the cooling rates W , i.e., for red detuning ($\Delta < 0$) there is cooling and for blue detuning ($\Delta > 0$) there is heating. The cooling rates saturate with increasing Rabi frequencies Ω_0 . These results coincide with those of Lindberg and Stenholm [9]. In the low-intensity case ($\Omega_0 \ll \Gamma$) these rates can be written as [6]

$$A_{\pm} = \Gamma[\alpha P(\Delta) + P(\Delta \pm \nu)]. \quad (50)$$

Here

$$P(\Delta) = \frac{\Omega_0^2}{2\Gamma^2} \frac{(\Gamma/2)^2}{(\Gamma/2)^2 + \Delta^2} \quad (51)$$

is the upper-state population for a (nonsaturated) two-level atom driven with frequency Ω_0 . As can be seen from Fig. 1(f), for the RW the lowest energy is reached for low intensities and for a detuning $\Delta = -\Gamma/2$.

For a trapped ion located at the node of a SW [$\varphi = \pi/2$, Figs. 1(a) and 1(b)] we find cooling for red detunings with cooling rates which do not saturate (i.e., as long as $\eta\Omega < \Gamma$ is fulfilled) and final energies which are independent of the applied Rabi frequency. Note that the final energy is a factor of 2 lower than for the RW at low intensities. This can be understood as follows: a trapped ion at the node of the SW does not encounter the laser at frequency ω_L since $\Omega_{\varphi=\pi/2} = 0$; however, due to the oscillatory motion of the ion there exist weak sidebands at frequencies $\omega_L \pm \nu$. Consequently, there is no

excitation and no saturation due to the (possibly strong) laser at frequency ω_L , so that the cooling rate increases with Ω_0^2 , and there is no diffusion. Explicitly, we find for all intensities Ω_0^2

$$A_{\pm} = \Gamma P(\Delta \pm \nu), \quad (52)$$

which should be compared with Eq. (50) for the RW case valid for low-intensities. The cooling rate W in the low intensity limit is identical with that of a SW. Since there is no saturation of the cooling rate it can be much higher than for the comparable case of a RW [cf. the scales in Figs. 1(e) and 1(a)]. Since A_+ and A_- show the same dependence on the Rabi frequency, the final energy $\langle n \rangle$ which is determined by the ratio A_+/W is independent of the Rabi frequency and is approximately a factor of 2 lower than for the RW case. Similarly, at the antinode of a SW we find in the low-intensity limit $A_{\pm} = \alpha\Gamma P(\Delta)$ and clearly no steady state can be reached since there is always heating due to the diffusion of the spontaneously scattered photons on resonance.

Interesting cooling and heating dynamics is observed at the SW's steepest gradient, i.e., for $\varphi = \pi/4$. As can be seen in Figs. 1(c) and 1(d), for low Rabi frequencies [actually for $\Omega_0 < \max(\nu, \Gamma)$] similar cooling results occur as for a RW [cf. the solid lines in Figs. 1(c) and 1(d)]. However, for large Rabi frequencies the ion experiences a strong dipole force due to the large gradient and laser cooling appears for blue detunings and heating for red detunings. This is the Sisyphus cooling effect which was found first in laser cooling of free atoms [13] and was recently calculated for trapped ions in a standing wave [16]. As can be seen from Figs. 1(c) and 1(d), the cooling rates are smaller for the given Rabi frequencies as compared to the RW case. However, inspection of Eq. (45) shows that the cooling rate does not saturate and increases with increasing Rabi frequency. Similarly, the final energy is determined by the applied Rabi frequency.

The turnover from red detuned cooling (for low Rabi frequencies) to blue detuned cooling is depicted in Fig. 2 in more detail. The curves *a*, *b*, and *c* represent the cooling rate W/η^2 (upper part) and the final energies (lower part) as a function of the detuning for the Rabi frequencies $\Omega_0 = 0.75\Gamma$ (curve *a*), $\Omega_0 = 1.25\Gamma$ (curve *b*), and $\Omega_0 = 1.75\Gamma$ (curve *c*). As the Rabi frequency increases, the cooling rate changes sign and blue cooling starts as is expected for Sisyphus cooling. The overall behavior of a trapped ion subject to cooling and heating in a SW at $\varphi = \pi/4$ can be seen in Fig. 3. Here, a contour plot of the final energy $\langle n \rangle$ (with contour lines $\langle n \rangle = 2, 4, \dots, 20$) is given as a function of the detuning Δ and Rabi frequency Ω_0 . For $\Omega_0 < \max(\Gamma, \nu)$ cooling appears for red detunings only and for $\Omega_0 > \max(\Gamma, \nu)$ blue cooling starts. Note that the detuning range for which Sisyphus cooling appears increases with increasing Rabi frequency, whereas the detuning range where red detuned cooling is still observed decreases in a corresponding way. A similar plot for the RW case would exhibit red detuned cooling only with contour lines, indicating that the final energy increases with increasing

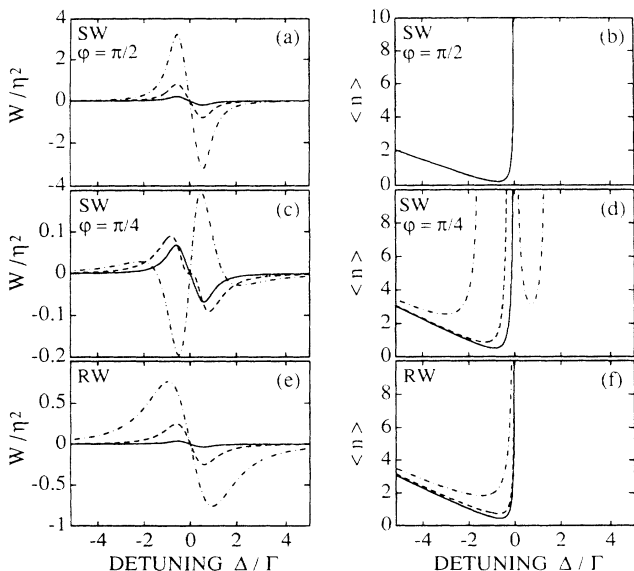


FIG. 1. Cooling rates W/η^2 and final energies $\langle n \rangle$ for a trapped two-level ion in a SW configuration at the node [$\varphi = \pi/2$ (a),(b)], at the point of the maximum gradient [$\varphi = \pi/4$ (c),(d)] and for a RW (e),(f) as a function of the laser detuning Δ/Γ . The parameters are $\Gamma = 1$, $\nu = 0.5$, and $\Omega_0 = 0.5\Gamma$ (solid line), $\Omega_0 = \Gamma$ (dashed line), $\Omega_0 = 2\Gamma$ (dashed-dotted line).

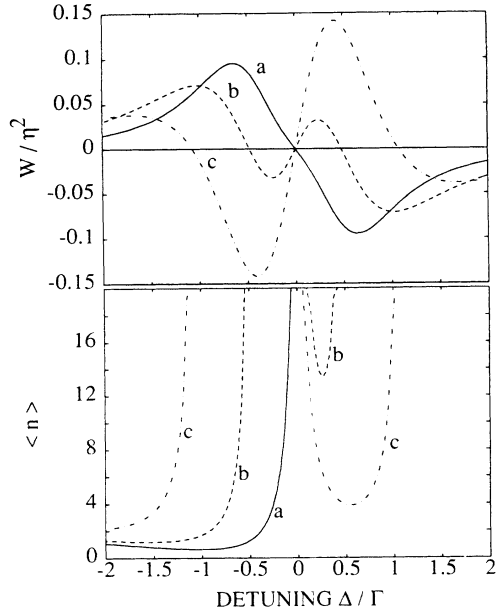


FIG. 2. Cooling rates W/η^2 (upper curves) and final energies $\langle n \rangle$ (lower curves) for a trapped two-level ion in a SW configuration at the point of the maximum gradient ($\varphi = \pi/4$). The parameters are $\Gamma = 1$, $\nu = 0.5$, and $\Omega_0 = 0.75\Gamma$ (curve a), $\Omega_0 = 1.25\Gamma$ (curve b), and $\Omega_0 = 1.75\Gamma$ (curve c).

Rabi frequency, as already discussed in the context of Fig. 1.

To exhibit the position dependence of a trapped ion in the SW, we show in Fig. 4 a contour plot of the final energy as a function of the detuning Δ and phases φ (with contour lines $\langle n \rangle = 2, 4, \dots, 20$) for a Rabi frequency $\Omega_0 = 6\Gamma$. As expected, for $\varphi = 0$ and $\varphi = \pi$ (i.e., at the antinodes) no cooling is observed, whereas red detuned cooling appears for phases in the vicinity

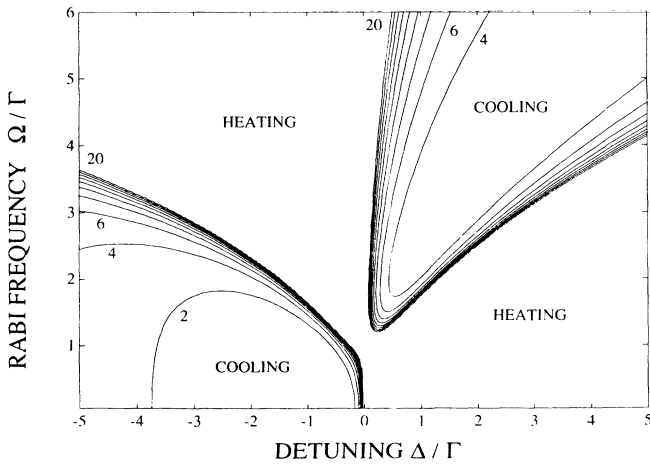


FIG. 3. Contour plot of the mean final energies (given by the mean quantum number $\langle n \rangle$) of a trapped ion at the maximum gradient of a SW configuration as a function of the laser detuning Δ/Γ for various Rabi frequencies Ω_0/Γ . The parameters are $\Gamma = 1$, $\varphi = \pi/4$ and each contour line indicates an increase in $\langle n \rangle$ by 2.

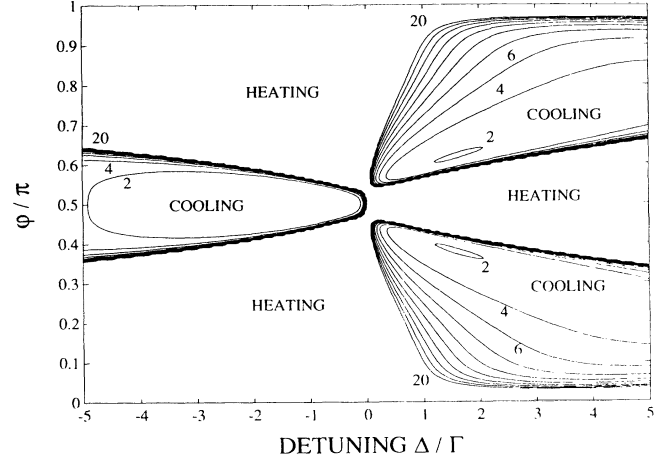


FIG. 4. Contour plot of the mean final energies (given by the mean quantum number $\langle n \rangle$) of a trapped ion in a SW configuration for a given Rabi frequency as a function of the laser detuning Δ/Γ for various phases φ . The parameters are $\Gamma = 1$, $\Omega_0 = 6\Gamma$ and each contour line indicates an increase in $\langle n \rangle$ by 2.

of $\varphi = \pi/2$ (i.e., at the node) and blue detuned cooling exists for phases around $\varphi = \pi/4$ (i.e., at the SW's maximum gradient). Note that the area where lowest $\langle n \rangle$ values are achieved is much larger for red detuned cooling than for blue detuned cooling. This is due to the fact that for blue detuned cooling the final energy is always determined by the applied Rabi frequency whereas at the node the final energy is independent of Ω_0 . Figure 5 shows a similar contour plot except that the Rabi frequency was chosen to be $\Omega_0 = \Gamma$. As expected, no blue detuned cooling appears and the area where red detuned cooling occurs is much wider than for $\Omega_0 = 6\Gamma$ since there is no heating due to the dipole forces. Again, at

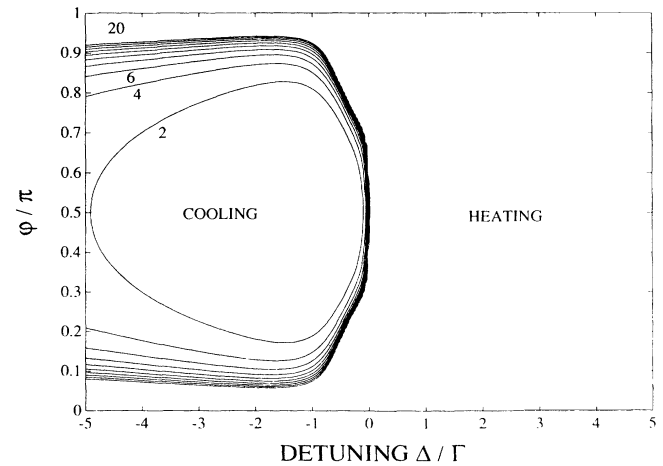


FIG. 5. Contour plot of the mean final energies (given by the mean quantum number $\langle n \rangle$) of a trapped ion in a SW configuration for a given Rabi frequency as a function of the laser detuning Δ/Γ for various phases φ . The parameters are $\Gamma = 1$, $\Omega_0 = 1\Gamma$ and each contour line indicates an increase in $\langle n \rangle$ by 2.

the antinodes ($\varphi = 0$ and $\varphi = \pi$) no cooling is observed.

In Fig. 6 we plot the transfer rates A_{\pm} as a function of the trap frequency ν . Note that $A_{-}(-\nu) = A_{+}(\nu)$. Thus for $\nu > 0$ the figure shows the transfer rate A_{-} ($n \rightarrow n - 1$) while the function for $\nu < 0$ corresponds to the transfer rate A_{+} ($n \rightarrow n + 1$). The subplots in Fig. 6 are (a) SW at the node ($\varphi = \pi/2$), (b) SW at the maximum gradient ($\varphi = \pi/4$), and (c) RW for the parameters are $\Omega_0 = 1, 4, 6\Gamma$, and $\Delta = -3\Gamma$. For a given ν the cooling rate is given by the difference $W = A_{-} - A_{+}$ and can be inferred from the asymmetry of the curves in Fig. 6 with respect to $\nu = 0$; the final energy is proportional to A_{+}/W . According to the discussion following Eq. (47) the ν dependence is equivalent to scanning the frequency of the probe beams $\omega_L \pm \nu$ corresponding to the motion-induced sidebands and the parameters in Fig. 6 correspond to an intense pump field at ω_L . Resonances as a function of ν appear at $\nu \approx 0$ and at the generalized Rabi frequency. In Fig. 6(a) there is only one resonance present since at the node of a SW there is no light field at frequency ω_L . In contrast, in Figs. 6(b) and 6(c) the center and the left peak are associated with a nonlinear mixing of the carrier at frequency ω_L with the sidebands $\omega_L \pm \nu$. The central peak is relevant for cooling in the weak-binding limit ($\nu < \Gamma$), whereas the left and

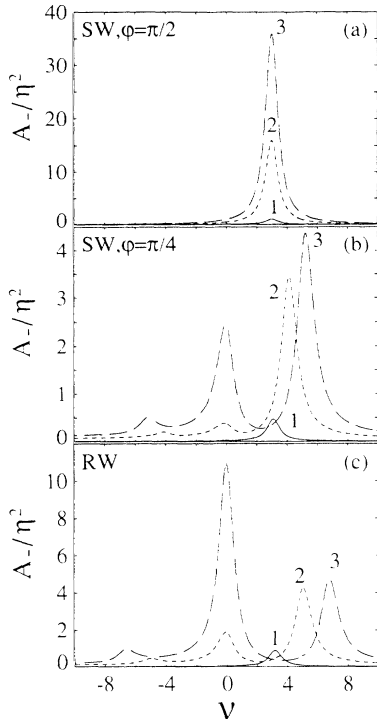


FIG. 6. Rates A_{-}/η^2 as a function of the trap frequency ν for a trapped ion in a SW configuration at the node [$\varphi = \pi/2$ (a)], at the point of the maximum gradient [$\varphi = \pi/4$ (b)] and for a RW (c), as a function of the laser detuning Δ/Γ . The parameters are $\Gamma = 1$, $\Omega_0 = \Gamma$ (1), $\Omega_0 = 4\Gamma$ (2), $\Omega_0 = 6\Gamma$ (3), and $\Delta = -3\Gamma$. For positive ν this represents the transition rate for $|n\rangle \rightarrow |n-1\rangle$ and for ν negative this represents the transition rate A_{+} for transitions from $|n\rangle \rightarrow |n+1\rangle$.

right peaks describe cooling in the strong-binding limit ($\nu > \Gamma$).

Finally, it is worth mentioning that all figures presented so far do not differ substantially from those obtained by solving numerically the (exact) master equation (1) (see Appendix B). Different results were found only for some parameters in the case of blue detuned cooling. An example is shown in Fig. 7, where we plot $\langle n \rangle$ as a function of the detuning Δ/Γ obtained by (i) numerical solution of master equation (1) (solid line) according to the procedure outlined in Appendix B, and (ii) from the rates A_{-} and A_{+} (dashed line) as given in Sec. II. The parameters in the figure are $\phi = \pi/4$, $\nu = 15\Gamma$, and $\Omega_0 = 40\Gamma$. As can be seen from the solid line, for some detuning there is no blue cooling in contrast to the calculations using the theory developed in Sec. II. The deviation is observed for detunings in the vicinity of $[(2\nu)^2 + \Omega_0^2]^{1/2}$. We interpret this result in the following way: as mentioned in the preceding section, cooling takes place when the absorption coefficient defined in (49) fulfills $A(\nu) > A(-\nu)$, i.e., when the sideband at frequency $\omega_L + \nu$ is more absorbed than that at frequency $\omega_L - \nu$. Taking into account higher orders in the LDL expansion, we find that there exist (very weak) sidebands centered at frequencies $\omega_L \pm 2\nu$ which are not considered in the treatment given in Sec. II. Usually they make a small contribution to the final energy in LDL. However, their contribution can become important when in first order $A(\nu) \approx A(-\nu)$. In this case, the first-order cooling rate is nearly zero and the absorption of photons of frequency $\omega_L - 2\nu$ (heating the ion) can dominate the cooling behavior. For a positive detuning this sideband frequency may be very close to the transition frequency of the TLS and consequently causes heating. This is predominant for $2\nu \approx (\Delta^2 + \Omega_0^2)^{1/2}$.

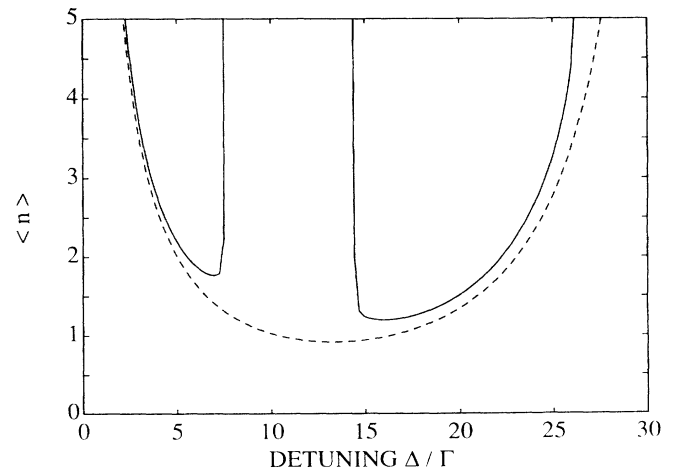


FIG. 7. Mean final quantum number $\langle n \rangle$ of a trapped two-level ion at the maximum gradient of a SW configuration as a function of the detuning Δ/Γ . The parameters are $\Gamma = 1$, $\Omega_0 = 40\Gamma$, and $\nu = 15\Gamma$. The dashed line shows the result obtained from A_{\pm} rates as given in Sec. II and the solid line represents the outcome of a numerical solution of the (exact) master equation according to the procedure given in Appendix B.

V. LASER COOLING OF A THREE-LEVEL SYSTEM IN A STANDING WAVE

In a recent paper by Wineland, Dalibard, and Cohen-Tannoudji [16] a single trapped three-level ion is considered to be laser cooled in a standing wave. They obtain in the LDL the evolution equation for the energy of the trapped particle. The authors calculate in particular the case where $\varphi = \pi/4$, i.e., the Sisyphus cooling at the point of the SW's maximum gradient, and they restrict their treatment to the case of a three-level atom.

In the following we compare the outcome of a calculation based on the theory presented in Sec. II with the results of Wineland, Dalibard, and Cohen-Tannoudji. For that reason we assume, analogous to Ref. [16], that the atom's internal structure is given by three levels, i.e., a ground state $|g\rangle$, an excited state $|e\rangle$, and an intermediate state $|r\rangle$ in between. The transition $|g\rangle \rightarrow |e\rangle$ is assumed to be an electric dipole transition excited by a standing-wave laser beam with Rabi frequency Ω_φ whose frequency is blue detuned with respect to the g - e resonance. Level $|e\rangle$ is assumed to decay spontaneously at a rate $\Gamma = 2\gamma$ both to the intermediate state $|r\rangle$ (with branching fraction β) and to the ground state [with branching fraction $(1-\beta)$]. Occupation in level $|r\rangle$ is assumed to be transferred (incoherently) back to level $|g\rangle$ with a rate $R_{r \rightarrow g}$.

In order to derive the coefficients A_- and A_+ that define master equation (26) we need the optical Bloch equations for the three-level atom at rest. For the particular three-level system described above they read as

$$\begin{aligned} \frac{d}{dt}\rho_g &= 2\gamma(1-\beta)\rho_e + R_{r \rightarrow g}\rho_r - \frac{\Omega_\varphi}{2}\langle\sigma_y\rangle, \\ \frac{d}{dt}\rho_e &= -2\gamma\rho_e + \frac{\Omega_\varphi}{2}\langle\sigma_y\rangle, \\ \frac{d}{dt}\rho_r &= 2\gamma\beta\rho_e - R_{r \rightarrow g}\rho_r, \\ \frac{d}{dt}\langle\sigma_x\rangle &= -\gamma\langle\sigma_x\rangle + \Delta\langle\sigma_y\rangle, \\ \frac{d}{dt}\langle\sigma_y\rangle &= -\Omega_\varphi(\rho_e - \rho_g) - \gamma\langle\sigma_y\rangle - \Delta\langle\sigma_x\rangle, \end{aligned} \quad (53)$$

where ρ_g , ρ_e , and ρ_r are the populations of levels $|g\rangle$, $|e\rangle$, and $|r\rangle$, respectively, Δ denotes the detuning, and $\langle\sigma_x\rangle$ and $\langle\sigma_y\rangle$ are the quadrature components of the atomic polarization for the transition $|g\rangle \rightarrow |e\rangle$. In the steady state the solution of Eqs. (53) is found to be

$$\begin{aligned} \rho_g^{\text{SS}} &= \left(\gamma^2 + \Delta^2 + \frac{\Omega_\varphi^2}{4}\right)P^{-1}, \\ \rho_e^{\text{SS}} &= \frac{\Omega_\varphi^2}{4}P^{-1}, \\ \rho_r^{\text{SS}} &= \frac{\Omega_\varphi^2}{2} \frac{\beta\gamma}{R_{r \rightarrow g}}P^{-1}, \\ \langle\sigma_x\rangle_{\text{SS}} &= \Delta\Omega_\varphi P^{-1}, \\ \langle\sigma_y\rangle_{\text{SS}} &= \gamma\Omega_\varphi P^{-1}, \end{aligned} \quad (54)$$

where now

$$P = \gamma^2 + \Delta^2 + \frac{\Omega_\varphi^2}{2} + \frac{\Omega_\varphi^2}{2} \frac{\beta\gamma}{R_{r \rightarrow g}}.$$

With this solution we find the diffusion coefficient D defined in (28) that reads as

$$D = \alpha[\rho_e^{\text{SS}}(\eta_{eg}^2\gamma(1-\beta) + \eta_{er}^2\gamma\beta) + \rho_r^{\text{SS}}\eta_{rg}^2R_{r \rightarrow g}/2], \quad (55)$$

where η_{ij} are the (small) Lamb-Dicke parameters. We calculate the spectrum

$$\int_0^\infty e^{i\nu t} \langle\sigma_x(t)\sigma_x(0)\rangle dt,$$

for the pumped transition $|g\rangle \rightarrow |e\rangle$ with Eqs. (53) and using the quantum regression theorem. Eventually, we obtain for the coefficients A_- and A_+

$$\begin{aligned} A_-(\nu) &= 2\eta_{eg}^2 \left(\frac{\Omega_0 \sin \varphi}{2}\right)^2 \\ &\times \text{Re} \left[\frac{\Delta\{i(\rho_g - \rho_e) + (\Omega_\varphi/2)[\sigma_x M(\nu) + i\sigma_y L(\nu)]\} + [\gamma - i\nu - (\Omega_\varphi^2/2)L(\nu)](\rho_g + \rho_e)}{\Delta^2 + (\gamma - i\nu)[\gamma - i\nu - (\Omega_\varphi^2/2)L(\nu)]} \right] + 2D, \\ A_+(\nu) &= A_-(-\nu), \end{aligned} \quad (56)$$

where

$$\begin{aligned} L(\nu) &= \frac{1}{R_{r \rightarrow g} - i\nu} \left(-1 + \frac{2\gamma(1-\beta) - R_{r \rightarrow g}}{2\gamma - i\nu} \right) - \frac{1}{2\gamma - i\nu}, \\ M(\nu) &= \frac{1}{R_{r \rightarrow g} - i\nu} \left(1 + i\frac{2R_{r \rightarrow g}}{\nu} + \frac{2\gamma(1-\beta) - R_{r \rightarrow g}}{2\gamma - i\nu} \right) - \frac{1}{2\gamma - i\nu}. \end{aligned}$$

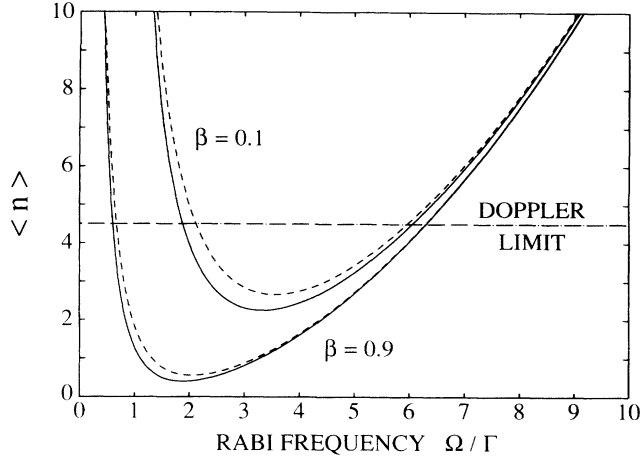


FIG. 8. Mean final quantum number $\langle n \rangle$ of a trapped three-level ion at the maximum gradient of a SW configuration as a function of the Rabi frequency of the laser cooling transition. The parameters are $\Delta = 10$ (blue detuning), $\Gamma = 1$, $\nu = 0.1$, $R_{r \rightarrow g} = 0.01$. The solid lines show the results according to the theory developed in Sec. II, the dashed lines are calculated from (58). The dashed-dotted line indicates the Doppler limit for these parameters.

The calculations of Wineland, Dalibard, and Cohen-Tannoudji are based on the assumption that the rate $R_{r \rightarrow g}$, the frequency ν , the decay constant Γ , and the detuning Δ obey the following relation

$$R_{r \rightarrow g} \ll \nu \ll \Gamma \ll \Delta. \quad (57)$$

In case that inequality holds, the final energy of the trapped ion is derived to be

$$E_{SS} = \frac{\nu}{2} \left(\frac{\Omega_\varphi^2}{4\Delta\nu} + \frac{4\Delta\nu}{\beta\Omega_\varphi^2} \right). \quad (58)$$

Figure 8 shows the final mean quantum number $\langle n \rangle$ as derived from (32) using A_- and A_+ given by (56) as a function of the Rabi frequency Ω_0 (solid lines). In order to compare this calculation with the result given by (58) we chose the parameters $R_{r \rightarrow g} = 0.01\gamma$, $\nu = 0.1\gamma$, $\Gamma = 1$, $\Delta = 10\gamma$ in accordance with condition (57). The dashed lines show the results according to [16].

Note first the remarkable agreement between the results. We have verified this agreement when conditions (57) are fulfilled. Note also that the minimum energy reached for the curves with $\beta = 0.9$ is much smaller than that of the Doppler cooling limit $E \sim \gamma$. However, as soon as the condition (57) is violated, deviations occur which tend to be smaller for higher Rabi frequencies.

VI. CONCLUSIONS

In this paper we have studied theoretically laser cooling of trapped ions in standing- and running-wave configurations, where the ions are assumed to be spatially localized on the scale of the laser wavelength (Lamb-Dicke limit). For the center-of-mass distribution of the ion a

master equation was derived using an adiabatic elimination procedure for a multilevel system in the LDL, valid for a general trapping potential. An essential step in the formulation of this master equation is the expression of the transition rates between the trap levels in terms of internal correlation functions for quadrature components of the atomic polarization.

Explicit solutions of the master equation were obtained for a harmonic trapping potential and two- and three-level systems in running and standing waves. For the two-level system located at the node of the standing wave we find final temperatures, which are a factor of 2 lower than the limit for a running wave, and cooling rates which do not saturate with the laser intensity. At the point of maximum gradient of the standing-wave blue detuned cooling was found which is analogous to the Sisyphus cooling of free atoms due to dipole forces. For a three-level system we have used our techniques to study a model which has been discussed very recently by Wineland, Dalibard, and Cohen-Tannoudji [16], and found agreement with these results within the limits of their approximation.

The theoretical tools developed in this paper open the prospect to calculate in a straightforward way the cooling rates and final energies for complicated *multilevel* ions in traps.

ACKNOWLEDGMENTS

The authors gratefully acknowledge discussions with J. Cooper, A.S. Parkins, and D. Wineland. J.I.C. and R.B. thank JILA for hospitality. The work at JILA is supported in part by the National Science Foundation. The work of W.D.P. is supported in part by the Office of Naval Research. R.B. was supported in part by the Deutsche Forschungsgemeinschaft.

APPENDIX A

In this appendix we derive the master equation (19) starting from Eq. (17). We also specialize this equation for a harmonic trap to obtain (26). As we are interested only in the evolution of the external degrees of freedom, we trace Eq. (17) over the internal states. On the other hand, it can be shown that for any internal operator X

$$\text{Tr}_I(X\mathcal{P}^i\rho) = \langle X \rangle_{SS}\mu, \quad (A1)$$

where μ is the reduced density operator defined in the text. Then, we find

$$\frac{d}{dt}\mu = \text{Tr}_I\{\mathcal{P}\mathcal{L}_2\mathcal{P} + \mathcal{P}\mathcal{L}_1(-\mathcal{L}_0)^{-1}\mathcal{L}_1\mathcal{P}\rho\}. \quad (A2)$$

The first term in Eq. (A2) is readily calculated and gives

$$\begin{aligned} & \frac{i}{2}\langle F' \rangle_{SS}\mathcal{P}^e[\hat{R}^2, \mu] \\ & + \alpha \sum_{i,j} \gamma_{ji} k_{ij}^2 \langle \sigma_{ii} \rangle_{SS} [2\hat{R}(\mathcal{P}^e\mu)\hat{R} - \hat{R}^2(\mathcal{P}^e\mu) - (\mathcal{P}^e\mu)\hat{R}^2]. \end{aligned} \quad (A3)$$

The derivation of the last term is more involved. We start using the properties of the Laplace transformation to express

$$\begin{aligned} \text{Tr}_I[\mathcal{P}\mathcal{L}_1(-\mathcal{L}_0)^{-1}\mathcal{L}_1\mathcal{P}\rho] \\ &= \int_0^\infty dt \text{Tr}_I[\mathcal{P}\mathcal{L}_1 e^{\mathcal{L}_0 t} \mathcal{L}_1 \mathcal{P}\rho] \\ &= \int_0^\infty dt \mathcal{P}^e \mathcal{L}_{1E} e^{\mathcal{L}_{0E} t} \\ &\quad \times [\mathcal{L}_{1E} \mathcal{P}^e \text{Tr}_I(F e^{\mathcal{L}_{0I} t} F \mathcal{P}^i \rho) \\ &\quad - \mathcal{P}^e \text{Tr}_I(F e^{\mathcal{L}_{0I} t} \mathcal{L}_{1I} \mathcal{P}^i \rho) \hat{R}], \end{aligned}$$

where for the last equality we have used the facts that the internal and external operators commute and $\text{Tr}_I(\mathcal{L}_{1I} \dots) = 0$.

The factors which appear inside the parentheses can be found using the quantum regression theorem,

$$\text{Tr}_I(F e^{\mathcal{L}_{0I} t} F \mathcal{P}^i \rho) = \langle F(t) F(0) \rangle_{\text{SS}} \mu, \quad (\text{A4})$$

$$\text{Tr}_I(F e^{\mathcal{L}_{0I} t} \mathcal{L}_{1I} \mathcal{P}^i \rho) = i \langle [F(t), F(0)] \rangle_{\text{SS}} \mu,$$

where, as usual,

$$\langle F(t) F(0) \rangle_{\text{SS}} = \lim_{\tau \rightarrow \infty} \langle F(t + \tau) F(\tau) \rangle. \quad (\text{A5})$$

In addition, given that

$$\begin{aligned} e^{\mathcal{L}_{0E} t} \mathcal{L}_{1E} \mu &= -i [(e^{\mathcal{L}_{0E} t} \hat{R}), \mu], \\ e^{\mathcal{L}_{0E} t} \mu \hat{R} &= \mu e^{\mathcal{L}_{0E} t} \hat{R}, \end{aligned}$$

and $\hat{R}(t) = e^{\mathcal{L}_{0E} t} \hat{R}$ is the Heisenberg operator of \hat{R} in the potential, we find the master equation (19).

For a harmonic trapping potential we repeat this derivation of the master equation by projecting on the Liouville subspaces $k = 0, \pm 1, \dots$ according to (25). Using (24) and (23), we find

$$\begin{aligned} \frac{d}{dt} u(\sigma^j, \lambda_1, \lambda_2) &= -i\nu \left(-\lambda_1 \frac{\partial}{\partial \lambda_1} + \lambda_2 \frac{\partial}{\partial \lambda_2} \right) u(\sigma^j, \lambda_1, \lambda_2) + i \frac{\Delta}{2} u([\sigma^j, \sigma_z], \lambda_1, \lambda_2) \\ &\quad - i \frac{\Omega_0}{4} [e^{-\lambda_2 \eta} e^{i\varphi} u(\sigma^j \sigma_x, \lambda_1 + \eta, \lambda_2 + \eta) - e^{-\lambda_1 \eta} e^{i\varphi} u(\sigma_x \sigma^j, \lambda_1 + \eta, \lambda_2 + \eta) \\ &\quad + e^{\lambda_2 \eta} e^{-i\varphi} u(\sigma^j \sigma_x, \lambda_1 - \eta, \lambda_2 - \eta) - e^{\lambda_1 \eta} e^{-i\varphi} u(\sigma_x \sigma^j, \lambda_1 - \eta, \lambda_2 - \eta)] \\ &\quad + \gamma 2\theta(\lambda_1 - \lambda_2, \eta) u(\sigma^+ \sigma^j \sigma^-, \lambda_1, \lambda_2) - u([\sigma^j, \sigma^+ \sigma^-]_+, \lambda_1, \lambda_2), \end{aligned} \quad (\text{B3})$$

where now

$$\theta(\lambda, \eta) = \frac{1}{2\eta} \int_{-\eta}^{\eta} d\eta' W \left(\frac{\eta'}{\eta} \right) e^{\eta' \lambda}, \quad (\text{B4})$$

and $W(x)$ has been defined in Sec. II.

Partial differential equations (B3) may be transformed in a set of infinite ordinary differential equations by making the ansatz

$$u(\sigma^j, \lambda_1, \lambda_2) = \sum_{n,m=0}^{\infty} \lambda_1^n \lambda_2^m u_{n,m}^j, \quad (\text{B5})$$

where the coefficients $u_{n,m}^j$ are given by

$$\begin{aligned} \frac{d}{dt} \mu_k &= -i \left(\nu - \frac{\langle F' \rangle_{\text{SS}}}{2M\nu} \right) [a^\dagger a, \mu_k] \\ &\quad + D(a\mu_k a^\dagger - a^\dagger a \mu_k + a^\dagger \mu_k a - a a^\dagger \mu_k + \text{H.c.}) \\ &\quad - \{S(-\nu)[a, [a^\dagger, \mu_k]] + S(\nu)[a^\dagger, [a, \mu_k]] \\ &\quad + T(-\nu)[a, \mu_k a^\dagger] + T(\nu)[a^\dagger, \mu_k a]\}, \end{aligned}$$

where μ_k is the density operator in the subspace k , and D has been defined in (28), $S(\nu)$ in (27), and

$$T(\nu) = \frac{1}{2M\nu} \int_0^\infty dt e^{i\nu t} \langle [F(t), F(0)] \rangle_{\text{SS}}.$$

Using the properties of the commutators between a and a^\dagger , we find (26).

APPENDIX B

In this appendix we show the method we have used to solve numerically the exact master equation (1) for a TLS interacting with a laser SW in a harmonic potential. This master equation is given by

$$\begin{aligned} \frac{d}{dt} \rho &= -i\nu [a^\dagger a, \rho] + \frac{1}{2} i \Delta [\sigma_z, \rho] \\ &\quad - i \frac{\Omega_0}{4} \left[\sigma_x \left(e^{i\varphi} e^{i\eta(a^\dagger + a)} + e^{-i\varphi} e^{-i\eta(a^\dagger + a)} \right), \rho \right] \\ &\quad + \gamma (2\sigma^- \tilde{\rho} \sigma^+ - \sigma^+ \sigma^- \rho - \rho \sigma^+ \sigma^-), \end{aligned} \quad (\text{B1})$$

where all the terms have been defined in Sec. II. To solve Eq. (B1) we define the characteristic functions by

$$u(\sigma^j, \lambda_1, \lambda_2, t) = \text{Tr} \left[e^{i\lambda_1 a^\dagger} e^{i\lambda_2 a} \sigma^j \rho(t) \right], \quad (\text{B2})$$

where $\{\sigma^j, j = 0, 1, 2, 3\} = \{1, \sigma_x, \sigma_y, \sigma_z\}$. Knowledge of $u(\sigma^j, \lambda_1, \lambda_2, t)$ gives all information about the evolution. Substituting this definition in the master equation (B1) we find the following evolution equation for $u(\sigma^j, \lambda_1, \lambda_2, t)$

$$u_{n,m}^j = \frac{i^{n+m}}{n!m!} (a^\dagger)^n a^m \sigma^j. \quad (\text{B6})$$

Taking into account the relations

$$\begin{aligned} e^{\mp \lambda_1 \eta} u(\sigma^j, \lambda_1 \pm \eta, \lambda_2 \pm \eta) &= \sum_{n,m} \lambda_1^n \lambda_2^m L_{n,m,j}^{1\pm}, \\ e^{\mp \lambda_1 \eta} u(\sigma^j, \lambda_1 \pm \eta, \lambda_2 \pm \eta) &= \sum_{n,m} \lambda_1^n \lambda_2^m L_{n,m,j}^{2\pm}, \\ \frac{1}{2\eta} \int_{-\eta}^{\eta} d\eta' \left[1 + \left(\frac{\eta'}{\eta} \right)^2 \right] e^{\eta'(\lambda_1 - \lambda_2)} u(\sigma^j, \lambda_1, \lambda_2) &= \sum_{n,m=0}^{\infty} \lambda_1^n \lambda_2^m M_{n,m,j}, \end{aligned}$$

where we have defined

$$\begin{aligned} L_{n,m,j}^{1\pm} &= \sum_{a=0}^{\infty} \sum_{b=m}^{\infty} u_{a,b}^j (\pm\eta)^{(b-m)} \binom{b}{m} N_{n,a}^{\pm}, \\ L_{n,m,j}^{2\pm} &= \sum_{a=n}^{\infty} \sum_{b=0}^{\infty} u_{a,b}^j (\pm\eta)^{a-n} \binom{a}{n} N_{m,b}^{\pm}, \\ M_{n,m,j} &= \sum_{c=0}^n \sum_{d=0}^m u_{c,d} (-1)^{2a-b} \binom{2a}{b} \eta^{2a} \left[\frac{1}{(2a+1)!} + \frac{1}{(2a+3)!} \right], \\ N_{x,y}^{\pm} &= \sum_{i=0}^{\min(x,y)} (-1)^{x-i} \frac{(\pm\eta)^{x+y-2i}}{(x-i)!} \binom{y}{i}, \end{aligned}$$

one finds the following infinite set of differential equations:

$$\begin{aligned} \dot{u}_{n,m}^0 &= i\nu(n-m)u_{n,m}^0 - i\frac{\Omega_0}{4}e^{-\eta^2/2} [e^{i\varphi}(L_{n,m,1}^{2+} - L_{n,m,1}^{1+}) + e^{-i\varphi}(L_{n,m,1}^{2-} - L_{n,m,1}^{1-})] \\ &\quad + \gamma \left[\frac{3}{4}(M_{n,m,0} + M_{n,m,3}) - (u_{n,m}^0 + u_{n,m}^3) \right], \\ \dot{u}_{n,m}^1 &= i\nu(n-m)u_{n,m}^1 + \Delta u_{n,m}^1 - i\frac{\Omega_0}{4}e^{-\eta^2/2} [e^{i\varphi}(L_{n,m,0}^{2+} - L_{n,m,0}^{1+}) + e^{-i\varphi}(L_{n,m,0}^{2-} - L_{n,m,0}^{1-})] - \gamma u_{n,m}^1, \\ \dot{u}_{n,m}^2 &= i\nu(n-m)u_{n,m}^2 - \Delta u_{n,m}^2 + i\frac{\Omega_0}{4}e^{-\eta^2/2} [e^{i\varphi}(L_{n,m,3}^{2+} + L_{n,m,3}^{1+}) + e^{-i\varphi}(L_{n,m,3}^{2-} + L_{n,m,3}^{1-})] - \gamma u_{n,m}^2, \\ \dot{u}_{n,m}^3 &= i\nu(n-m)u_{n,m}^3 - i\frac{\Omega_0}{4}e^{-\eta^2/2} [e^{i\varphi}(L_{n,m,2}^{2+} + L_{n,m,2}^{1+}) + e^{-i\varphi}(L_{n,m,2}^{2-} + L_{n,m,2}^{1-})] \\ &\quad - \gamma \left[\frac{3}{4}(M_{n,m,0} + M_{n,m,3}) + (u_{n,m}^0 + u_{n,m}^3) \right]. \end{aligned}$$

We have solved these equations in the steady state with an iteration method, assuming $u_{n_0, m_0}^j = 0$ for certain n_0 and m_0 , and checking that the results did not change when n_0 and m_0 were increased.

* Present address: Departamento de Física Aplicada, Facultad de Ciencias Químicas, Universidad de Castilla-La Mancha, 13071 Ciudad Real, Spain.

† Permanent address: I. Institut für Experimentalphysik, Jungiusstrasse 9, D-2000, Hamburg 36, Germany.

- [1] D.J. Wineland, W.M. Itano, and R.S. VanDyck, Jr., *Adv. At. Mol. Phys.* **19**, 135 (1983).
- [2] See, for example, special issue on "the physics of trapped ions," edited by R. Blatt, P. Gill, and R.C. Thompson, *J. Mod. Opt.* 1992 (to be published).
- [3] D. Wineland and H.G. Dehmelt, *Bull. Am. Phys. Soc.* **20**, 637 (1975).
- [4] W. Neuhauser, M. Hohenstatt, P.E. Toschek, and H.G. Dehmelt, *Phys. Rev. Lett.* **41**, 233 (1978); D.J. Wineland, R.E. Drullinger, and F.L. Walls, *ibid.* **40**, 1639

(1978).

- [5] P.E. Toschek, in *New Trends in Atomic Physics Vol. I*, Proceedings of the Les Houches Summer School, Session XXXVIII, edited by G. Grynberg and R. Stora (North-Holland, Amsterdam 1984), p. 381.
- [6] S. Stenholm, *Rev. Mod. Phys.* **58**, 699 (1986).
- [7] R. Blatt, in *Fundamental Systems in Quantum Optics*, Proceedings of the Les Houches Summer School, Session LIV, edited by J. Dalibard, J.M. Raymond, and J. Zinn-Justin (Elsevier, New York, in press).
- [8] D.J. Wineland and W.M. Itano, *Phys. Rev. A* **20**, 1521 (1979); W.M. Itano and D.J. Wineland, *ibid.* **25**, 35 (1982).
- [9] M. Lindberg and S. Stenholm, *J. Phys. B* **17**, 3375 (1985).

- [10] M. Lindberg and J. Javanainen, *J. Opt. Soc. Am. B* **3**, 1008 (1986).
- [11] F. Diedrich, J.C. Bergquist, W.M. Itano, and D.J. Wineland. *Phys. Rev. Lett.* **62**, 403 (1989).
- [12] See articles in *Laser Cooling and Trapping* [*J. Opt. Soc. Am. B* **6** (1989)].
- [13] J. Dalibard and C. Cohen-Tannoudji, *J. Opt. Soc. Am. B* **2**, 1707 (1985).
- [14] P.D. Lett, R.N. Watts, C.I. Westbrook, W.D. Phillips, P.L. Gould, and H. J. Metcalf, *Phys. Rev. Lett.* **61**, 1069 (1988); J. Dalibard and C. Cohen-Tannoudji, *J. Opt. Soc. Am. B* **6**, 2023 (1989); P.J. Ungar, D.S. Weiss, E. Riis, and S. Chu, *ibid.* **6**, 2058 (1989).
- [15] A. Aspect, E. Arimondo, R. Kaiser, N. Vansteenkiste, and C. Cohen-Tannoudji, *Phys. Rev. Lett.* **61**, 826 (1988); A. Aspect, E. Arimondo, R. Kaiser, N. Vansteenkiste, and C. Cohen-Tannoudji, *J. Opt. Soc. Am. B* **6**, 2112 (1989).
- [16] D. Wineland, J. Dalibard, and C. Cohen-Tannoudji, *J. Opt. Soc. Am. B* **9**, 32 (1992).
- [17] Nan Yu, Hans Dehmelt, and Warren Nagourney, *Proc. Natl. Acad. Sci. U.S.A.*, **86**, 5671 (1989).
- [18] C.W. Gardiner, *Quantum Noise* (Springer-Verlag, Berlin, 1991).
- [19] In (26) there is no reference to the index k [see Eq. (25)] since for a harmonic oscillator the master equation is identical for each eigenvalue λ_k .
- [20] For a discussion of probe absorption see P. Meystre and M. Sargent III, *Elements of Quantum Optics* (Springer-Verlag, Berlin, 1990), Chap. 15-4, p. 410.